ACS OMEGA

http://pubs.acs.org/journal/acsodf

Article

Synthesis of Organic–Inorganic Hybrids Based on Perovskite-like Bismuth Titanate $H_2K_{0.5}Bi_{2.5}Ti_4O_{13}·H_2O$ and *n*-Alkylamines

Iana A. Minich, Oleg I. Silyukov,* Veronika V. Gak, Evgeny V. Borisov, and Irina A. Zvereva

Cite This: *ACS Omega* 2020, 5, 8158–8168

Read Online

ACCESS | Metrics & More | Article Recommendations | Supporting Information

ABSTRACT: New organic–inorganic hybrids have been synthesized by the intercalation of *n*-alkylamines (methylamine, ethylamine, *n*-propylamine, *n*-butylamine, *n*-hexylamine, and *n*-octylamine) into the structure of the protonated and hydrated form of the perovskite-like layered titanate $H_2K_{0.5}Bi_{2.5}Ti_4O_{13}·H_2O$ ($HKBT_4·H_2O$). The possibility of the synthesis of the hybrid materials was studied in a wide range of conditions. It was found that interlayer water plays a crucial role in the formation of intercalated hybrids. The obtained compounds were characterized with powder X-ray diffraction analysis; Raman, IR, and NMR spectroscopies; thermogravimetry (TG), TG coupled with mass spectrometry, and CHN analyses; and scanning electron microscopy. It was suggested that the intercalated *n*-alkylamines exist in the form of alkylammonium ions forming a paraffin-like bilayer with an average tilting angle of ∼77.5°. The obtained $HKBT_4×RNH_2$ compounds contain 0.4–0.7 *n*-alkylamine molecules per formula unit as well as the varied amount of intercalated water. By gentle heating, they can be obtained as dehydrated forms, which are thermally stable up to 250 °C.

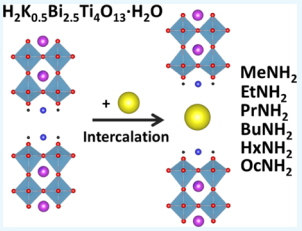

1. INTRODUCTION

Layered perovskite-like oxides are mixed oxide ceramics formed by perovskite slabs interleaved with cations and structural units. Perovskites are widely studied as perspective materials for a wide range of applications because of their physical and chemical properties such as superconductivity,[1,2] colossal magnetoresistance,[3] and catalytic and photocatalytic activity.[4−7] Among them, bismuth-containing structures draw special attention. They are considered as a lead-free ferroelectric[8−10] and multiferroic materials.[11] They may perform as effective photoanode materials for photoelectrochemical water splitting,[12] and Bi^{3+}/Mn^{4+} codoping has been recently applied as an effective approach for the preparation of red-emitting phosphors for white light-emitting diodes.[13,14]

One of the unique features of layered compounds is the possibility of the introduction of molecules into the interlayer space.[15] In the case of inorganic layered compounds, the most interesting process is the intercalation of organic molecules into the inorganic matrix, resulting in new organic–inorganic hybrid materials.[16−20] Such compounds combine physicochemical properties that are a superposition of the original inorganic compound and the introduced organic matter. According to the type of chemical bond between inorganic and organic parts, there are two main ways of formation hybrids with layered compounds: intercalation and grafting.[21] Intercalation is a reversible noncovalent introduction of organic molecules into the interlayer space proceeding usually by the acid–base or ion-exchange mechanism.[15,22,23] Covalent inorganic–organic hybrids may be produced by grafting reactions—intercalation of appropriate organic substances accompanied by the formation of covalent bonds.[24−26] Recently, a large number of works have been devoted to the study of metal halide inorganic–organic layered perovskite hybrids exhibiting interesting optoelectrical properties,[27,28] while much less attention has been paid to hybrids based on layered perovskite-like oxides.

Ion-exchangeable layered perovskite-like oxides are solid crystalline substances with a block-type structure in which perovskite slabs with a thickness of *n*-octahedra BO_6 (B = Ti, Nb, Ta, etc.) alternate with the so-called interlayer spaces containing alkali cations.[29] Such compounds have the ability to replace the interlayer cations of alkali metals by ion exchange with other cations, in particular, cations of other metals, complex cationic units, or protons, to obtain the so-called protonated forms. One of the significant features of protonated forms of perovskite-like oxides is their acidic properties, which allows the intercalation of organic bases into their interlayer space forming organic–inorganic hybrids. Such compounds can be interesting both on their own because of their physicochemical properties, such as photocatalytic activity,[30−32] and can be the basis for the creation of new materials by liquid-phase exfoliation.[7,33,34]

Among ion-exchangeable layered perovskites, the most widely studied compounds amenable to intercalation of organic molecules are protonated derivatives of Dion–Jacobson (DJ), Ruddlesden–Popper (RP), and Aurivillius

Received: January 30, 2020
Accepted: March 18, 2020
Published: March 30, 2020

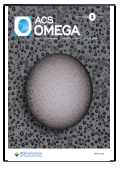

phases.[35] The most thoroughly studied among others in terms of intercalation and grafting of organic molecules are $HLaNb_2O_7$,[18,20,36−39] $HCa_2Nb_3O_{10}$,[24,40] $H_2CaTa_2O_7$,[39,41] and $H_2La_2Ti_3O_{10}$[42] compounds. Although the number of obtained protonated forms of layered perovskite-like oxides is limited, new such compounds are synthesized regularly.

Recently, Liu et al.[43] have synthesized a new n = 4 layered RP phase $K_{2.5}Bi_{2.5}Ti_4O_{13}$ (KBT_4) with mixed K/Bi co-occupancy on the perovskite A site showing stoichiometric hydration and amenable to form the protonated compound $H_2K_{0.5}Bi_{2.5}Ti_4O_{13}{\cdot}yH_2O$[44,45] by substitution of K^+ by H^+. The $H_2K_{0.5}Bi_{2.5}Ti_4O_{13}{\cdot}H_2O$ ($HKBT_4{\cdot}H_2O$) structure can be described as an alternation of perovskite slabs ($K_{0.5}Bi_{2.5}Ti_4O_{13}$) with interlayer protons and water molecules (Figure 1a).

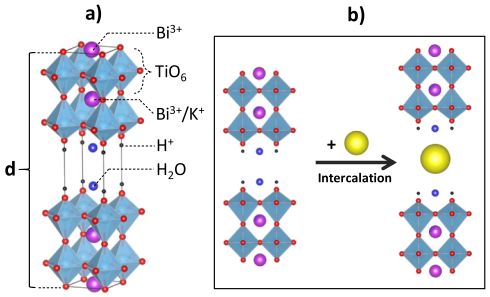

Figure 1. Schematic representation of $HKBT_4{\cdot}H_2O$ structure (a) and intercalation process (b). The d-value represents the basal spacing (interlayer distance along the c-axis).

This work presents a complex study on the behavior of protonated and hydrated forms of $H_2K_{0.5}Bi_{2.5}Ti_4O_{13}{\cdot}yH_2O$ obtained from $K_{2.5}Bi_{2.5}Ti_4O_{13}$ toward the intercalation (Figure 1b) of n-alkylamines with different numbers of carbon atoms (n_c) in alkyl chain, namely, methylamine, ethylamine, n-propylamine, n-butylamine, n-hexylamine, and n-octylamine, and the characterization of obtained hybrids in terms of their composition, structure, and thermal stability.

The previously studied hosts belonging to the RP phases (e.g., $H_2La_2Ti_3O_{10}$,[42] $H_2CaTa_2O_7$,[41] and $HLnTiO_4$[46]) and DJ phases ($HCa_2Nb_3O_{10}$[40] and $HLaNb_2O_7$[39]) are known to intercalate n-amines in solvothermal or microwave-assisted solvothermal conditions. In this work, various approaches have been considered in order to determine the optimal experimental conditions of amine intercalation into the interlayer space of $H_2K_{0.5}Bi_{2.5}Ti_4O_{13}{\cdot}yH_2O$.

There are two main factors that are reported to strongly affect the intercalation reactivity of protonated forms obtained from layered perovskites. The first one is the Brønsted acidity of interlayer protons, which is associated with the interlayer charge densities and depends on the nature of B-site and A-site cations. In addition, the second one is the sterical accessibility of the interlayer space,[47] which could be theoretically "tailored" by the preparation of various hydrated forms. As is already known, some phases show poor or no reactivity in intercalation reactions compared to other ones,[39,48,49] which is assumed to be the result of their irreversible dehydration. Considering the possibility of a strong influence of the interlayer water on the occurrence of amine intercalation reactions, both the as-prepared hydrated phase ($H_2K_{0.5}Bi_{2.5}Ti_4O_{13}{\cdot}H_2O$) and partly and fully dehydrated phases $H_2K_{0.5}Bi_{2.5}Ti_4O_{13}{\cdot}0.5H_2O$ and $H_2K_{0.5}Bi_{2.5}Ti_4O_{13}$ have been used for the experiments.

2. RESULTS AND DISCUSSION

2.1. Synthesis. *2.1.1. Protonation.* The protonated hydrated compound $H_2K_{0.5}Bi_{2.5}Ti_4O_{13}{\cdot}H_2O$ ($HKBT_4{\cdot}H_2O$) was successfully prepared from $K_{2.5}Bi_{2.5}Ti_4O_{13}$. The amount of intercalated water and the substitution degree of the as-prepared protonated form calculated from thermogravimetry (TG) data, energy-dispersive X-ray, and inductively coupled plasma (ICP) elemental analyses confirm the complete substitution of interlayer K^+ by H^+, and the amount of intercalated water was found to be ∼1 H_2O molecule per formula unit. Partially ($HKBT_4{\cdot}0.5H_2O$) and fully ($HKBT_4$) dehydrated forms were prepared by subsequent heating of $HKBT_4{\cdot}H_2O$. Figure 2 shows X-ray diffraction (XRD) data for

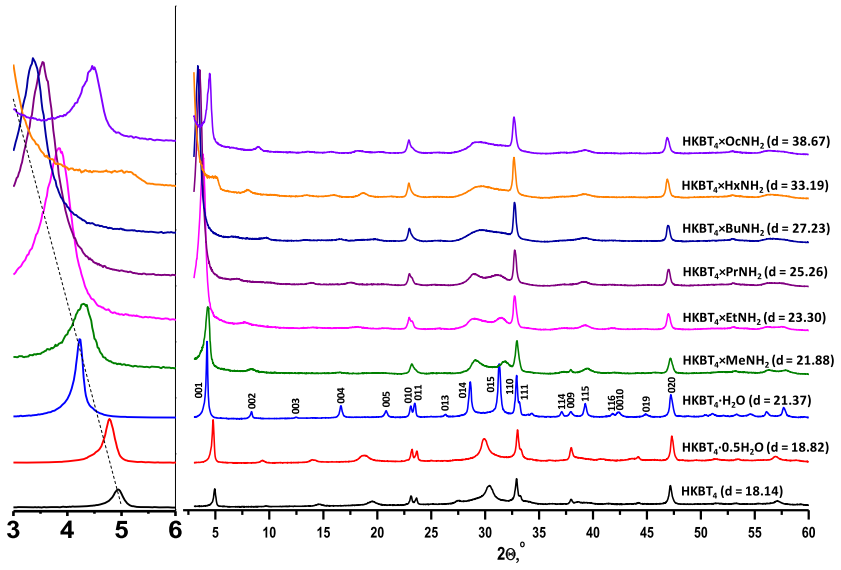

Figure 2. XRD patterns of hydrated and dehydrated forms of $HKBT_4$ and obtained n-alkylamine intercalated compounds $HKBT_4{\times}RNH_2$ together with calculated interlayer distances.

https://dx.doi.org/10.1021/acsomega.0c00424
ACS Omega 2020, 5, 8158−8168

the as-prepared $HKBT_4{\cdot}H_2O$ sample and dehydrated samples obtained by heat treatment at 90 °C for $HKBT_4{\cdot}0.5H_2O$ and 160 °C for $HKBT_4$. Their XRD patterns and lattice parameters are in accordance with previously reported data.[45]

2.1.2. Intercalation of Amines. A series of experiments of amine intercalation with varying conditions have been first carried out for three amines (methylamine, *n*-butylamine, and *n*-octylamine) (Table 3). Then, the optimal conditions with respect to the phase purity of the obtained samples, amine loading, and reaction time have been chosen and applied for the remaining three amines (ethylamine, *n*-propylamine, and *n*-hexylamine).

In the case of methylamine, the phase pure samples could be obtained in all tested conditions; however, intercalation does not lead to any significant changes in the interlayer space. TG measurements have been employed in order to estimate the amount of intercalated organic molecules in different conditions. It was found that methylamine is intercalated into $HKBT_4{\cdot}H_2O$ at 25 °C after 24 h of stirring, but the highest mass loss is achieved after 14 days of stirring. Similar mass losses could be reached, though, using heating at 60 °C for 24 h in order to optimize the reaction time, so the sample obtained in these conditions was used for further characterization.

In the case of *n*-butylamine, the intercalation leads to a significant change in the XRD pattern of the sample corresponding to the interlayer distance change. Reactions with concentrated *n*-butylamine (90−100%) may cause the formation of a side product surely resulted by dehydration of the initial form, while using 10 and 50% water solutions both leads to the formation of single-phase products. However, using 10% concentrated *n*-butylamine requires longer reaction time compared to 50% solutions. Unlike methylamine, the maximum amount of *n*-butylamine is readily intercalated into $HKBT_4{\cdot}H_2O$ by facile stirring at 25 °C in the shortest reaction time tested (24 h) using 50% water solution. The sample obtained at these reaction conditions has been used for further characterization.

In the case of *n*-octylamine, no water was added into suspension because of its low solubility in water. The attempts of direct intercalation of pure *n*-octylamine into hydrated $HKBT_4{\cdot}H_2O$ at room temperature have led to its dehydration. Considering the experiments with intercalation of *n*-butylamine into dehydrated forms (described later), it was assumed that once dehydrated in the presence of *n*-octylamine, $HKBT_4{\cdot}H_2O$ would not be able to intercalate it. The experiments with the *n*-octylamine solution in heptane showed that the single-phase sample could be obtained after 24 h of treatment at 80 °C. Additionally, longer reaction time (1 week) leads to the formation of the same phase with similar amine loading.

2.2. Characterization. The detailed characterization of organic−inorganic hybrids was carried out for six samples obtained by optimized methods. Namely, methylamine, ethylamine, and *n*-propylamine derivatives were obtained at 60 °C within 24 h. The *n*-butylamine derivative was prepared by facile suspending and stirring the as-prepared hydrated $HKBT_4{\cdot}H_2O$ powder in 50% water solution of *n*-butylamine at 25 °C for 24 h. Finally, hybrids with *n*-hexylamine and *n*-octylamine were prepared by 24 h treatment with 50% solution in *n*-heptane at 80 °C.

2.2.1. Powder XRD Analysis. As displayed in Figure 2, the XRD patterns show that because of the small molecular size, the intercalation of methylamine does not strongly affect the lattice parameters of the compound in respect to $HKBT_4{\cdot}H_2O$, and the slight changes obtained in the XRD patterns could be associated with the intercalation of methylamine or possible formation of different hydrated $HKBT_4$ compounds, so such changes cannot prove intercalation of methylamine without other characterization methods. However, in the case of n_c = 2−8 amines, the XRD patterns clearly indicate major structural changes that could be associated with the intercalation of big molecules into interlayer space.

Despite the fact that the obtained organic−inorganic samples show low crystallinity, the obtained *n*-alkylamine intercalated compounds could be indexed based on the index of the starting $HKBT_4{\cdot}H_2O$ compound, which can be well indexed in the primitive tetragonal cell with lattice parameters a, b = 3.85 Å and c = 18.14 Å (although a slightly better XRD pattern fit can be obtained using an orthorhombic *C*222 group or a *P*4 space group with a doubled c lattice parameter[45]). After the reaction of $HKBT_4{\cdot}H_2O$ with *n*-alkylamines, the (00*l*) reflection shifts to a lower 2-theta value, indicating the increase in interlayer distance and shows a gradual increase as larger amines are intercalated; the calculated interlayer distances are presented in Figure 2. Widening and low intensities of observed reflections are typical for such intercalated compounds and could be explained by the weakening of bonding between layers resulting in possible turbostratic stacking and interlayer distance deviations.[15,22] However, the preservation of sharp, intense reflections with indexes 010, 110, and 020 for the starting protonated form (without the contribution of c in *hkl*) indicates no significant structural changes in the perovskite slabs.

2.2.2. IR and Raman Spectroscopy. The Fourier transform infrared (FT-IR) and Raman spectra of the protonated hydrated form and organic−inorganic hybrids are shown in Figure 3. The appearance of characteristic bands at 1400−1600 and 2800−3000 cm^{-1} corresponding to NH_3^+ and C−H vibrations confirms the formation of organic−inorganic hybrids in all of the cases (including methylamine). In particular, the bands at the range 2800−3000 cm^{-1} are attributed to CH_2 symmetric stretching ν_s ($-CH_2-$), and the lower intensity bands at 1400−1550 cm^{-1} correspond to CH_2 asymmetric bending δ_{as} ($-CH_2-$) and NH_3^+ asymmetric bending δ_{as} ($-NH_3^+$).[50] The presence of NH_3^+ bands (and also the absence of characteristic to NH_2 group ν_s and ν_{as} bands in the region 3500−3300 cm^{-1}) implies the acid−base mechanism of amine intercalation into this protonated form, leading to the formation of cationic forms of amines in the interlayer space. In the IR spectra of $HKBT_4{\times}RNH_2$ derivatives, where R = Bu, Hx, and Oc, two major bands in the C−H stretching region were clearly exhibited, namely, the ν_{as} ($-CH_2-$) (~2918 cm^{-1}) and the ν_s ($-CH_2-$) (~2854 cm^{-1}) of CH_2 groups and also ν_{as} ($-CH_3$) (~2956 cm^{-1}) are visible. Because the frequency and width of ν_{as} ($-CH_2-$) are sensitive to the gauche/trans conformer ratio and the packing density of methylene chains, the appearance of sharp ν_{as} ($-CH_2-$) band and its frequency points to the all-trans conformation of *n*-alkyl chains in the interlayer space.[51] The broad band occurring in the 3100−3500 cm^{-1} range is produced by O−H stretching vibration, and the broad band near 1600 cm^{-1} is due to the bending vibration of H_2O molecule, suggesting the existence of interlayer water in the samples.

It should also be noted that the Raman spectrum of the *n*-octylamine intercalated sample shows a significantly enhanced

https://dx.doi.org/10.1021/acsomega.0c00424
ACS Omega 2020, 5, 8158−8168

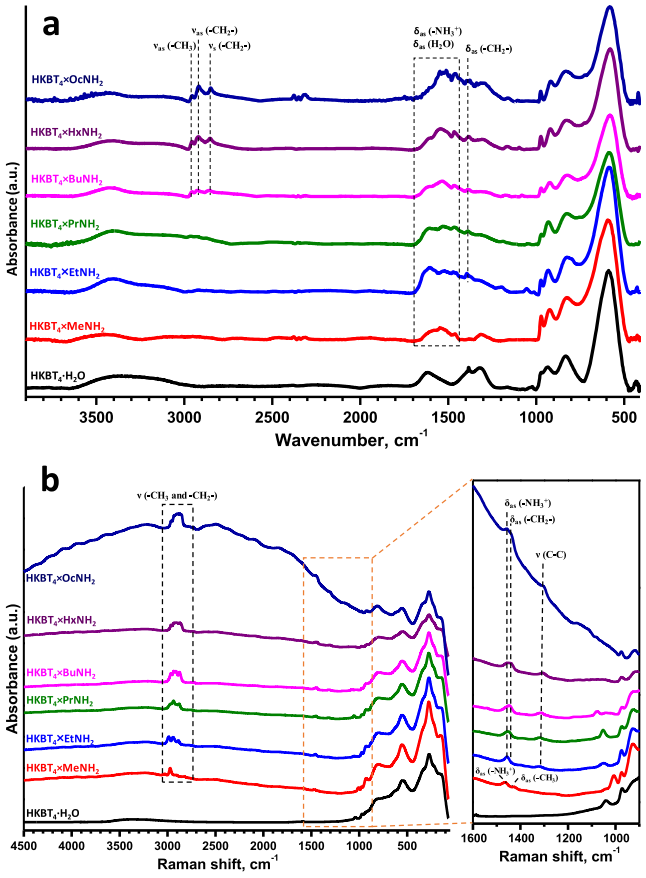

Figure 3. FT-IR (a) and Raman (b) spectra of obtained *n*-alkylamine intercalated compounds $HKBT_4{\times}RNH_2$ in comparison with the initial $HKBT_4{\cdot}H_2O$ compound.

and reproducible fluorescence compared to other samples at measurement conditions used. This motivated us to additionally examine the optical properties of the samples. As shown in Table 1 containing optical band gaps (Eg) of the samples,

Table 1. Absorption Characteristics of Initial Protonated Form and Inorganic−Organic Hybrids

sample	Eg, eV	λ_{max}, nm	sample	Eg, eV	λ_{max}, nm
$HKBT_4{\cdot}H_2O$	3.29	377	$HKBT_4{\times}BuNH_2$	3.17	391
$HKBT_4{\times}MeN_2$	3.17	391	$HKBT_4{\times}HxNH_2$	3.15	394
$HKBT_4{\times}EtNH_2$	3.19	389	$HKBT_4{\times}OcNH_2$	3.15	394
$HKBT_4{\times}PrNH_2$	3.19	389			

calculated from their diffuse reflectance spectra (Figure S1), intercalation of amines does not significantly affect the Eg and the corresponding maximum wavelengths λ_{max} of absorbed light. There is only a slight decrease in Eg values and a slight increase in the wavelengths λ_{max} of absorbed light for the hybrids in comparison with the protonated form, and in general, spectra do not differ from each other, which indicates that the enhanced fluorescence of $HKBT_4{\times}OcNH_2$ is not related to the optical properties of the sample and should be explained by other reasons.

2.2.3. ^{13}C NMR-MAS Spectroscopy. The solid-state ^{13}C MAS-NMR spectra of six hybrids are shown in Figure 4. The characteristic peak at 26 ppm for the methylamine-intercalated compound is shifted upfield compared to the raw methylamine (28 ppm), which indicates that methylamine is presented in the cationic form and the interaction between the inorganic matrix and methylamine takes place.[52] A similar shift of (A) and (B) carbon peak position is also observed for ethylamine (36.7 → 35, 18.8 → 14), *n*-propylamine (44.4 → 42, 27.3 → 22), *n*-butylamine (41.9 → 40, 36 → 30), *n*-hexylamine (42.4 → 40, 34.9 → 32), and *n*-octylamine (42.35 → 42, 34 → 30), which is in good agreement with the[13] C NMR spectra of the corresponding alkylammonium salts. In the case of *n*-butylamine hybrid, four signals could be attributed to four carbon atoms in different environments $NH_3^+{-}CH_2(A){-}CH_2(B){-}CH_2(C){-}CH_3(D)$ at 40(A), 30(B), 21(C), and 14(D) ppm. These results correlate well with previously presented results for *n*-butylamine-intercalated RP titanate $H_2La_2Ti_3O_{10}$[42] and Aurivillius-based tantalate $H_2Bi_{0.1}Sr_{0.85}Ta_2O_7$.[53] The spectrum of *n*-octylamine hybrid shows a multiplet in the range 34−30 ppm, which could be assigned to methylene units in the middle of the carbon chain [B,C (30); D,E (32); and F (34)]. Single peaks at 15 and 24 ppm account to methyl ($-CH_3$ (H)) and methylene ($-CH_2$ (G)) groups. The signal at ∼42 ppm corresponds to the CH_2 group in A position with respect to the—NH_3^+ group.[54] The splitting of this signal may be due to the presence of some part of *n*-octylamine in both cationic and neutral forms as well as because of different alkylammonium cation surroundings. It should be underlined that the MAS-NMR results confirm the assumption of the acid−base mechanism of the intercalation reaction, showing that amines are mostly presented in the interlayer space in their cationic forms which correlate well with the results of Raman and IR spectroscopies.

2.2.4. TG and CHN Analysis. TG analysis additionally confirms the intercalation of *n*-amines, as the total mass loss for all of the samples is higher than that for an initial protonated form (Figure 5). The total mass losses and compositions estimated using CHN and TG analyses are presented in Table 2. The amounts of amines intercalated in the compound were estimated from the carbon and nitrogen content obtained by CHN analysis, and the residual water content was calculated from TG analysis. As can be seen, the calculated compositions correspond to only 20−35% of the theoretical cation-exchange capacity (interlayer proton/amine ratio = 1:1), which is lower than for other reported *n*-alkylamine derivatives of RP titanates.[42,55] The absence of interlayer water in the octylamine sample, according to the calculation data, may explain the luminescence observed in this case during the measurements of Raman spectra (Figure 3).

In the case of all obtained hybrids, the thermal decomposition process is complex and includes three main stages. The first mass loss stage at temperature up to 350−400 °C most probably associated with the deintercalation and vaporization of water and organic molecules, as well as the decomposition of the protonated form itself. The samples heated up to 350−400 °C change their color from white to yellowish-brown probably because of the reduction of partial inorganic part by intercalated amines. At the second stage, a significant mass gain occurs apparently associated with oxidation processes and can be explained by the oxidation of the remaining organic part or as oxidation of reduced inorganic part (associated most probably with Ti^{4+}/Ti^{3+} or Bi^{3+}/Bi^0 redox transition). At the third stage, the final mass loss can be associated with decomposition of the remaining oxidized organic compounds and/or with their "burning" in an oxidative atmosphere. Despite the fact that the difference in the behavior

https://dx.doi.org/10.1021/acsomega.0c00424
ACS Omega 2020, 5, 8158−8168

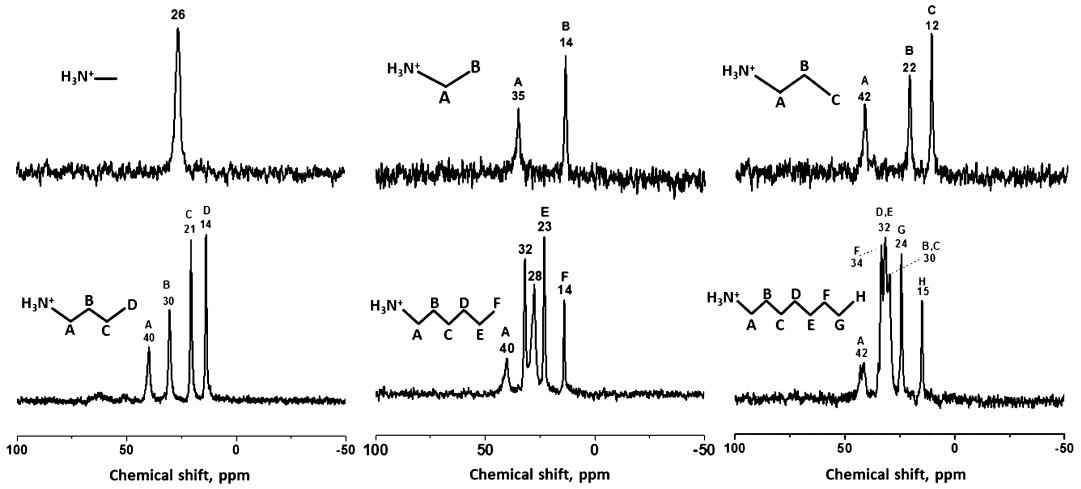

Figure 4. ^{13}C MAS-NMR spectroscopy for the obtained *n*-alkylamine intercalated compounds $HKBT_4{\times}RNH_2$.

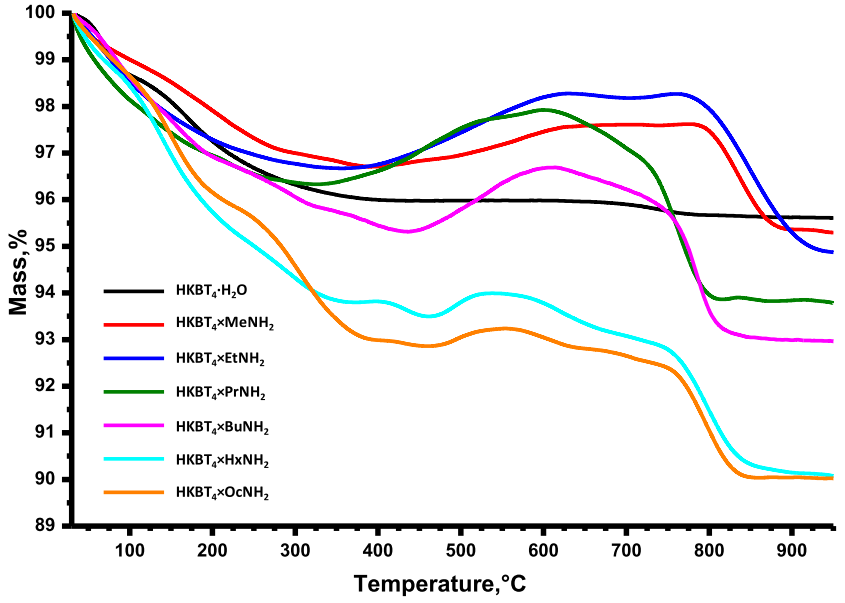

Figure 5. TG curves of the obtained *n*-alkylamine intercalated compounds $HKBT_4{\times}RNH_2$ in the air atmosphere in comparison with the initial $HKBT_4{\cdot}H_2O$ compound.

Table 2. Experimental and Calculated Composition Data of the Obtained Intercalated Compounds

	experimental				calculated		
sample	Δ*m*, %	C, %	N, %	C/N	estimated composition	C, %	N, %
$HKBT_4{\times}MeNH_2$	4.7	0.6	0.85	0.8:1	$H_2K_{0.5}Bi_{2.5}Ti_4O_{13}{\cdot}0.6MeNH_2{\cdot}0.6H_2O$	0.75	0.85
HKBT4×EtNH2	5.1	0.9	0.55	2.0:1	$H_2K_{0.5}Bi_{2.5}Ti_4O_{13}{\cdot}0.4EtNH_2{\cdot}0.9H_2O$	1.0	0.55
HKBT4×PrNH2	6.3	1.5	0.6	2.9:1	$H_2K_{0.5}Bi_{2.5}Ti_4O_{13}{\cdot}0.4PrNH_2{\cdot}1.1H_2O$	1.45	0.6
HKBT4×BuNH2	7.1	2.6	0.7	4.4:1	$H_2K_{0.5}Bi_{2.5}Ti_4O_{13}{\cdot}0.5BuNH_2{\cdot}0.9H_2O$	2.4	0.7
HKBT4×HxNH2	9.9	4.7	0.7	7.4:1	$H_2K_{0.5}Bi_{2.5}Ti_4O_{13}{\cdot}0.5HxNH_2{\cdot}1.0H_2O$*	3.55	0.7
HKBT4×OcNH2	10.0	6.5	0.95	8.3:1	$H_2K_{0.5}Bi_{2.5}Ti_4O_{13}{\cdot}0.7OcNH_2$	6.5	0.95

*Relatively high carbon content can be explained by the presence of residual solvent (approximately 0.1 molecules of *n*-heptane per formula unit).

of the samples during thermal decomposition is obvious, there is no single explanation for this based only on the composition data or synthetic conditions of the samples.

2.2.5. TG Coupled with Mass Spectrometry. The mechanism of dehydration and decomposition and the thermal stability of organic−inorganic composites were studied by TG coupled with mass spectrometry of eliminated gases in an argon atmosphere (Figure 6). The results suggest that unlike $H_2La_2Ti_3O_{10}$-based amine hybrids,[55] the *n*-butylamine-intercalated $HKBT_4$ is rather stable under heat treatment. Its thermal decomposition may be separated into two main stages: elimination of water at low temperatures and decomposition of *n*-butylamine at higher temperatures. The first stage at 30−230 °C shows the elimination of water (major ion current at this range is $m/z = 18$), which is the result of dehydration. The further heating from 230 to 450 °C first leads to the detection

https://dx.doi.org/10.1021/acsomega.0c00424
ACS Omega 2020, 5, 8158−8168

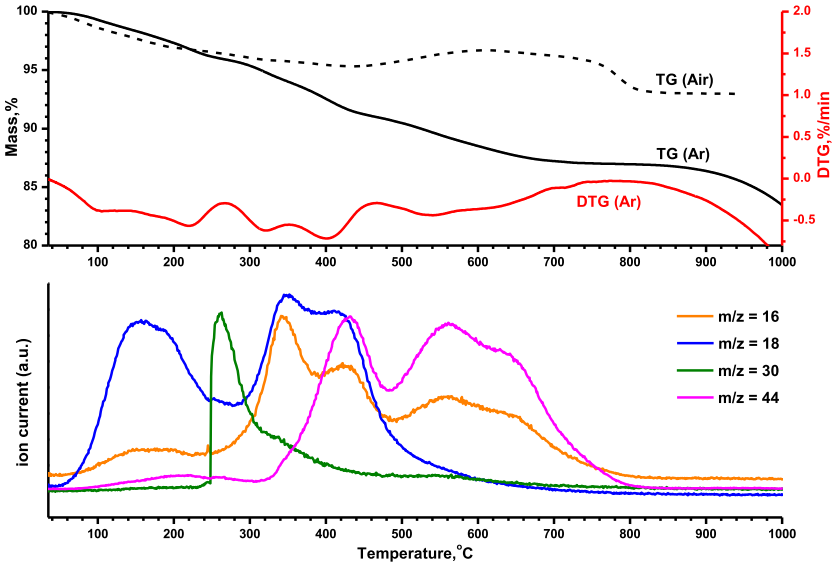

Figure 6. Results of TG-MS analysis of evolved gases during $HKBT_4{\times}BuNH_2$ heating in the Ar atmosphere.

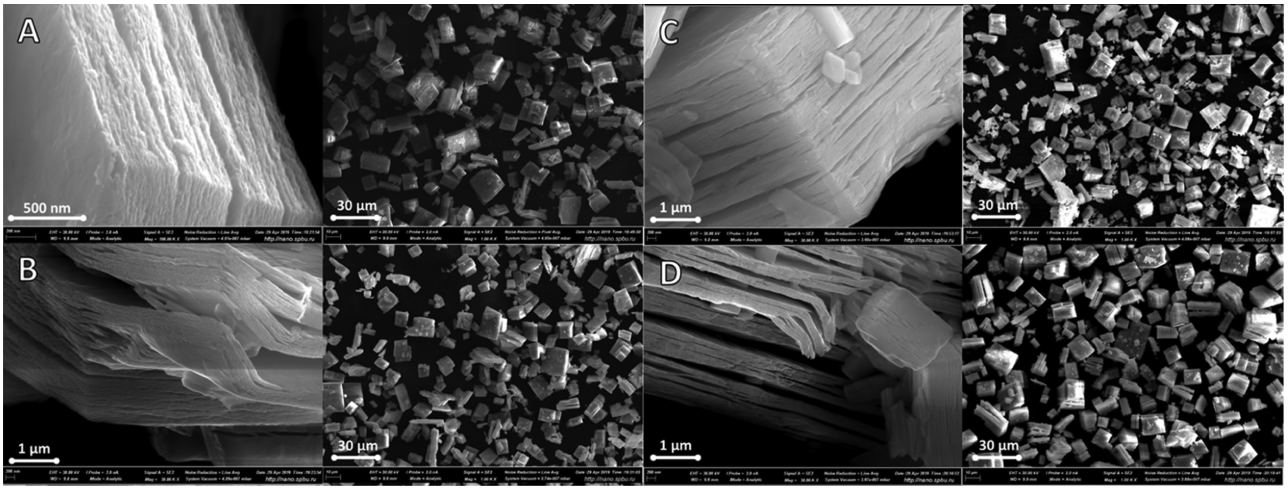

Figure 7. SEM images for the (a) protonated form of $HKBT_4{\cdot}H_2O$ and organic−inorganic hybrids (b) $HKBT_4{\times}MeNH_2$, (c) $HKBT_4{\times}BuNH_2$, and (d) $HKBT_4{\times}OcNH_2$.

of ion current m/z = 30 in evolved gases associated with elimination of intercalated amine ($CH_2NH_2^+$) and then (starting from temperatures about 300 °C) the increase in the contribution of m/z = 18 and 16 is detected, which could be attributed to water elimination. It should be noted that the ion current m/z = 16 is too high at this stage to be explained only as water elimination. At the same time, it could not be associated with CO_2 elimination because the related ion current with m/z = 44 is negligible at this stage. A possible explanation of this phenomenon could be related to the elimination of lattice oxygen or the elimination of NH_3 (associated with m/z = 16—NH_2^+). Heating the sample at temperatures higher than 350 °C leads to the elimination of CO_2 (m/z = 44) and water (m/z = 18), which continues up to ∼500 °C; after that, the mass loss on TG is mainly associated with CO_2 elimination (m/z = 44, 16). The last two processes in Ar atmosphere could be explained as the reaction between organic and inorganic parts of the hybrid material accompanied by the reduction of metal (Bi^{3+} and Ti^{4+}) cations; hence, the mass loss at temperature higher 800 °C (without detection of ion currents) can be associated with metallic Bi evaporation (attention! A repetition of such TG coupled with mass spectrometry (TG-MS) experiment in an inert atmosphere is strongly discouraged; the precipitated bismuth can cause damage to the platinum parts of the device!).

To sum up, dehydration, which is expected to be similar in Ar and Air atmospheres, is completed at 230 °C, and the further mass loss at higher temperatures may be attributed to the elimination of *n*-butylamine and decomposition of the protonated form itself.

2.2.6. Scanning Electron Microscopy. The morphologies of the obtained protonated and intercalated forms were studied by scanning electron microscopy (SEM) (Figure 7). The as-prepared protonated forms have a plate-like shape, which is typical for layered compounds. The obtained microcrystals have relatively big sizes of 5−10 μm in two directions and partly split into thin stacked sheets in the third direction. The intercalation of amines leads to the further splitting and swelling of the platelets, though, the major shape and sizes have remained. Such behavior could explain the observed peak widening on the XRD patterns of the obtained hybrid compounds.

https://dx.doi.org/10.1021/acsomega.0c00424
ACS Omega 2020, 5, 8158−8168

2.3. Influence of Interlayer Water on Hybrid Formation. The reported structural characterization of $HKBT_4{\cdot}H_2O$ showed that it may be indexed in tetragonal *P*4. The partial dehydration at 90 °C leads to the decrease of *c* parameter (and therefore the interlayer distance), accompanied by displacement of perovskite blocks in *a* and *b* directions, leading to I-type stacking sequence. Both of these factors are likely to result in lower proton accessibility and therefore lower reactivity in intercalation reactions. The complete dehydration at 160 °C and formation of $HKBT_4$ leads to a further decrease in the interlayer distance with the displacement of perovskite blocks in the *c* direction as implied by calculated lattice parameters.[45]

In order to examine the influence of interlayer water in the host compound on its activity in intercalation reactions, a partly dehydrated $HKBT_4{\cdot}0.5H_2O$ and fully dehydrated $HKBT_4$ samples have been used for intercalation reactions with methylamine and *n*-butylamine. The conditions tested are presented in Table 3. The treatment of both dehydrated samples with 50% water solution of *n*-butylamine at room temperature and under heating (60−80 °C) did not show any changes in the XRD patterns, which indicate that no reaction takes place. These results are in accordance with the previously reported assumptions.[48,49] Methylamine has a smaller molecular size, and as reported earlier, it could be directly intercalated into a three-layered RP titanate $H_2La_2Ti_3O_{10}$ with a I-type stacking sequence,[55] which allows the assumption of the possibility of its intercalation in partly or fully dehydrated protonated forms $HKBT_4{\cdot}0.5H_2O$ and $HKBT_4$. However, the experiments showed that it could not be intercalated into these phases nor in room temperature conditions, nor upon heating.

Table 3. Reaction Conditions Examined for the Preparation of Organic−Inorganic Hybrids

precursor	reaction medium	temperature, °C	duration
	Intercalation of Methylamine		
$HKBT_4{\cdot}H_2O$	38% solution in water	20	24 h−2 weeks
		60	24 h−1 week
$HKBT_4{\cdot}0.5H_2O$	38% solution in water	20	24 h−1 week
		60, 80	
$HKBT_4$	38% solution in water	20	24 h−1 week
		60, 80	
	Intercalation of Ethylamine		
$HKBT_4{\cdot}H_2O$	50% solution in water	60	24 h
	Intercalation of *n*-Propylamine		
$HKBT_4{\cdot}H_2O$	50% solution in water	60	24 h
	Intercalation of *n*-Butylamine		
$HKBT_4{\cdot}H_2O$	10, 50, 90% solution in water, 100% *n*-butylamine	20, 60	24 h−1 week
	50% solution in water	60	24−72 h
$HKBT_4{\cdot}0.5H_2O$	50% solution in water	20	24 h−1 week
		60, 80	
$HKBT_4$	50% solution in water	20	24 h−1 week
		60, 80	
	Intercalation of *n*-Hexylamine		
$HKBT_4{\cdot}H_2O$	50% solution in *n*-heptane	80	24 h
	Intercalation of *n*-Octylamine		
$HKBT_4{\cdot}H_2O$	100%; 50% solution in *n*-heptane	20, 60	24 h−1 week
	50% solution in *n*-heptane	80	24 h−1 week

2.4. Discussion. Intercalated organic derivatives $HKBT_4{\times}RNH_2$ can be synthesized using a hydrated and protonated RP compound $HKBT_4{\cdot}H_2O$ as the starting material but not its partially ($HKBT_4{\cdot}0.5H_2O$) or completely dehydrated ($HKBT_4$) forms, suggesting a strong influence of interlayer water molecules on chemical activity upon intercalation. Despite the attempts to optimize the synthetic procedure, we were unable to obtain compounds with an organic content higher than 0.35 per proton of the initial compound. This is far less than the theoretic capacity equal of approximately one amine molecule per proton limited by steric factors as opposed to previously obtained results for other RP titanates.[42,46,55] The other difference between the obtained $HKBT_4{\times}RNH_2$ compounds and the previously reported *n*-alkylamine derivatives of perovskite-like layered compounds is the thermal decomposition behavior. First of all, because of the high thermal stability of its organic parts, synthesized hybrids, apparently, may be obtained in an anhydrous (dehydrated) form.

Comparing the interlayer distance change between $HKBT_4$ and the obtained *n*-amine-intercalated compounds $HKBT_4{\times}RNH_2$ with n_c = 1, 2, 3, 4, 6, and 8 (Δd = 3.74, 5.16, 7.12, 9.09, 15.11, and 20.53 Å correspondingly) with the linear size of the intercalated amine molecules (2.94, 4.16, 5.44, 6.69, 9.22, and 11.75 Å correspondingly), we can see that the calculated distance changes are higher than the linear size of the single amine molecule. Because several types of linear amine arrangements are known for layered structures,[22] there could be different explanations of such interlayer space widening. Taking into account the results of Raman, IR, and ^{13}C NMR spectroscopy characterization, suggesting the all-trans conformation of the *n*-alkyl chains, we can assume a bilayer arrangement model for intercalated amines. Because the length of *n*-alkyl chains in the all-trans conformation increases by 0.127 nm per CH_2 unit, the calculated linear relationship between the interlayer distance and the number of carbon atoms in *n*-alkylamine (Figure 8a) can be explained by a tilted bilayer arrangement of *n*-alkyl chains in the interlayer with a tilt angle of ∼77.5°. This value is much higher than that previously observed for the *n*-alkylamine derivatives of RP phase $H_2SrTa_2O_7$ (51°) with a similar amount of intercalated molecules (∼25% of the theoretical cation-exchange capacity) and bilayer chain arrangement,[56] but it can be compared to *n*-alkylamine-intercalated RP $H_2W_2O_7$[57] (∼71.6°), $H_{1.8}[Sr_{0.8}Bi_{0.2}Ta_2O_7]$[58] (∼60°), DJ niobate $HCa_2Nb_3O_{10}$[40] (∼62.3°), and also to *n*-alcohol-grafted derivatives of RP tantalate $H_2CaTa_2O_7$ (∼70°)[41] and titanate $H_2La_2Ti_3O_{10}$ (∼75°).[42]

Taking into account the *n*-alkylamine chain size and an assumption that during intercalation of *n*-alkylammonium cations occupy cavities on the (100) surface of the perovskite-like slabs as it was previously reported for other layered perovskite compounds,[57,58] a simple structural model with tilted bilayer arrangement of alkyl chains can be proposed (Figure 8b).

The nature of enhanced and reproducible fluorescence of the $HKBT_4{\times}OcNH_2$ sample is not clear. As we have shown, it is not related to the differences in the optical properties of the samples and should be explained by other reasons. We suppose that one of the possible reasons may be the presence of a higher organic carbon content in this sample, as it is known

https://dx.doi.org/10.1021/acsomega.0c00424
ACS Omega 2020, 5, 8158−8168

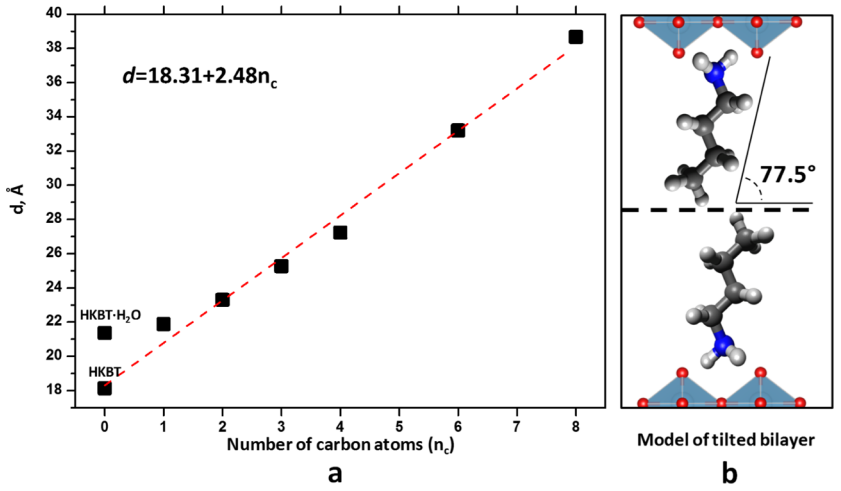

Figure 8. (a) Correlation between interlayer distance and the number of carbon atoms (n_c) in *n*-alkylamine and (b) schematic representation of the proposed $HKBT_4$×RNH_2 alkyl chain arrangement (on the example of $HKBT_4$×$BuNH_2$).

that the organic substance fluorescence is one of the limitations of the Raman spectroscopy method, and typically, the longer-wavelength lasers are used for organic substances (NIR and IR lasers) in order to reduce the fluorescence. From the other side, bismuth-containing compounds, including complex oxides and layered oxides, are already known to exhibit luminescent properties,[59] so the observed luminescence may not be directly connected to the organic content and type. We assume that it may actually be in one way or another connected with changes in the composition (organic content and type and water content), structure (change in the interlayer distance), or morphology of the sample (in particular, partial splitting or presence of an exfoliated phase). However, more complex research is needed for rigorous conclusions.

3. CONCLUSIONS

Intercalation reactions of a new RP-layered perovskite-like bismuth titanate protonated form with *n*-alkylamines have been studied for the first time. It was shown that it readily undergoes the intercalation of *n*-alkylamines in moderate and enhanced temperatures. The optimal conditions for the preparation of organic−inorganic hybrids have been determined. It was shown that intercalated amines are mainly presented in the interlayer space in cationic forms. The study of the impact of interlayer water on intercalation reactivity showed that it is a crucial factor for proceeding intercalation reactions.

4. EXPERIMENTAL SECTION

4.1. Materials. KNO_3 (Vekton, 99.9%), Bi_2O_3 (Vekton, 99.9%), and TiO_2 (Vekton, 99.9%) were dried at 200, 600, and 1000 °C, respectively. Methylamine (38% water solution, Chemical line), *n*-ethylamine (70% water solution, Merck), *n*-propylamine (Sigma-Aldrich, 98%), *n*-butylamine (99.9%, Chemical line), *n*-hexylamine (Sigma-Aldrich, 99.9%), *n*-octylamine (Vekton, 99.9%), and *n*-heptane (ECOS, 99.9%) were used as received.

4.2. Preparation of Inorganic Hosts. The starting oxide $K_{2.5}Bi_{2.5}Ti_4O_{13}$ and its protonated forms were obtained according to the previously described procedures. $K_{2.5}Bi_{2.5}Ti_4O_{13}$ host was synthesized by conventional ceramic technique from Bi_2O_3, TiO_2, and KNO_3.[43] The amounts of oxides were taken in stoichiometric molar ratios, and KNO_3 was taken with 20% excess to compensate for its loss due to the volatilization. The mixture was ball milled at 600 rpm for 100 min, pelletized into ∼2 g tablets, and calcined at 750 °C for 8 h twice with intermediate regrinding. The protonated hydrated form $H_2K_{0.5}Bi_{2.5}Ti_4O_{13}·H_2O$ ($HKBT_4·H_2O$) was obtained by suspending 2 g of alkali form in 40 mL of 1 M HNO_3 and stirring it at 25 °C for 1 week.[44] Then, the obtained suspension was centrifuged, washed with distilled water, and dried at room temperature over CaO. The partly and fully dehydrated forms $H_2K_{0.5}Bi_{2.5}Ti_4O_{13}·0.5H_2O$ ($HKBT_4·0.5H_2O$) and $H_2K_{0.5}Bi_{2.5}Ti_4O_{13}$ ($HKBT_4$) were prepared by heat treatment of the as-prepared hydrated form at 90 and 160 °C for 30 min correspondingly.[45]

4.3. Reactions with *n*-Amines. In order to determine the optimal conditions for the preparation of amine-intercalated hybrids ($HKBT_4$×RNH_2), the series of experiments in various conditions were carried out, including varying the reaction temperature, time, and medium. The examined experimental conditions are presented in Table 3. Room-temperature reactions were carried out by suspending the $HKBT_4$ powder in a solution of amines and stirring at 25 °C for 1−14 days in sealed glass vessels. Reactions with heating were carried out at 60/80 °C for 1−7 days using ∼50 mL Teflon-lined vessels inserted in stainless steel autoclaves. The volumes of suspensions were taken according to the 80% occupancy rate of the vessel. The amine-treated powders were collected by filtration (poly(tetrafluoroethylene) membrane filters, 0.20 μm porosity diameter) and washed with acetone (in case of amines with n_c = 1−4) and hexane (in case of amines with n_c = 6 and 8).

4.4. Instrumentation. The formation of new phases was observed by powder XRD analysis with a Rigaku MiniFlex II diffractometer (Cu Kα radiation, λ = 0.15406 nm, 2θ = 3 − 60°, and scan speed = 10° min^{-1}). The intercalation of organic molecules into interlayer space was confirmed by Raman and FT-IR-spectroscopies and MAS-NMR spectroscopy. The FT-IR spectra of the samples were recorded with an FT-IR spectrometer IR Prestige-21, with a resolution of 1 cm^{-1} in the range of 4000−400 cm^{-1}, using the KBr pellet technique. Raman spectra were collected by a Bruker SENTERRA spectrometer in the range of 100−4000 cm^{-1} using a 488

https://dx.doi.org/10.1021/acsomega.0c00424
ACS Omega 2020, 5, 8158−8168

nm 4 mW laser with a 25 μm aperture, and the spectrum accumulation time was 60 s. In order to control the possible decomposition of the samples influenced by the laser beam, the measurements have been repeated six times in one point. Solid-state NMR spectroscopy was performed by a Bruker AVANCE III 400 WB spectrometer at operating frequencies 100.64 MHz (for ^{13} C). Powder samples were placed in a zirconium oxide rotor with an external diameter of 4 mm and rotated at a frequency of 12.5 kHz at a magic angle to the direction of a constant magnetic field. To register the spectra on ^{13}C nuclei, a cross-polarization excitation pulse sequence was used (CP/MAS technique). For the CP/MAS technique, the contact time was 2 ms, the relaxation delay time was 5 s, and the number of accumulations was 12,000. Tetramethylsilane was used as an external reference. The investigation of dehydration and decomposition of organic−inorganic hybrids were performed by means of TG analysis (TG 209 F1 Libra, Netzsch) in the flow of synthetic dry air (50 mL/min) at a heating rate of 10°C/min. The quantitative composition of the obtained hybrids was estimated from the results of TG analysis and CHN analysis. The mechanism of dehydration and decomposition of the samples was estimated using the results of TG−MS in an argon atmosphere (STA 449 F1 Jupiter, Netzsch and QMS 403C Aëolos), and studies were performed in the flow of argon (50 mL/min) at a heating rate of 20°C/min. The CHN analysis was performed using a Euro EA3028-HT analyzer.

■ ASSOCIATED CONTENT

Supporting Information

The Supporting Information is available free of charge at https://pubs.acs.org/doi/10.1021/acsomega.0c00424.

Diffuse reflectance spectra of initial protonated titanates and their inorganic−organic hybrids; DRS performed on a Shimadzu UV-2550 spectrometer with ISR-2200 integrating sphere attachment; obtained DRS used to calculate the optical band gaps (Eg) of the samples presented in Table 1 (PDF)

■ AUTHOR INFORMATION

Corresponding Author

Oleg I. Silyukov − *Institute of Chemistry, St. Petersburg State University, 198504 St. Petersburg, Russia;* orcid.org/0000-0003-1235-727X; Email: oleg.silyukov@spbu.ru

Authors

Iana A. Minich − *Institute of Chemistry, St. Petersburg State University, 198504 St. Petersburg, Russia*

Veronika V. Gak − *Institute of Chemistry, St. Petersburg State University, 198504 St. Petersburg, Russia*

Evgeny V. Borisov − *Center for Optical and Laser Materials Research, St. Petersburg State University, 198504 St. Petersburg, Russia*

Irina A. Zvereva − *Institute of Chemistry, St. Petersburg State University, 198504 St. Petersburg, Russia;* orcid.org/0000-0002-6898-3897

Complete contact information is available at: https://pubs.acs.org/10.1021/acsomega.0c00424

Author Contributions

The manuscript was written through the contributions of all authors. All authors have given approval to the final version of the manuscript.

Notes

The authors declare no competing financial interest.

■ ACKNOWLEDGMENTS

This study was supported by the Russian Foundation for Basic Research (grant no. 18-03-00915). I.A.M. also thank the Russian Foundation for Basic Research for its financial support (grant no. 19-33-90050). The authors are also grateful to Saint Petersburg State University Research Park: Center for X-ray Diffraction Studies, Center for Optical and Laser Materials Research, Center for Chemical Analysis and Materials Research, Center for Thermal Analysis and Calorimetry, Magnetic Resonance Research Centre, Interdisciplinary Center for Nanotechnology, and SDBSWeb: https://sdbs.db.aist.go.jp (National Institute of Advanced Industrial Science and Technology).

■ REFERENCES

(1) Liu, Y.; Mao, Z.-Q. Unconventional Superconductivity in Sr_2RuO_4. *Phys. C* **2015**, *514*, 339−353.

(2) Ogino, H.; Sato, S.; Kishio, K.; Shimoyama, J.-i. Relationship between Crystal Structures and Physical Properties in Iron Arsenides with Perovskite-Type Layers. *Phys. Procedia* **2012**, *36*, 722−726.

(3) Moritomo, Y.; Asamitsu, a.; Kuwahara, H.; Tokura, Y. Giant Magnetoresistance of Manganese Oxides with a Layered Perovskite Structure. *Nature* **1996**, *380*, 141−144.

(4) Takata, T.; Furumi, Y.; Shinohara, K.; Tanaka, A.; Hara, M.; Kondo, J. N.; Domen, K. Photocatalytic Decomposition of Water on Spontaneously Hydrated Layered Perovskites. *Chem. Mater.* **1997**, *9*, 1063−1064.

(5) Rodionov, I. A.; Zvereva, I. A. Photocatalytic Activity of Layered Perovskite-like Oxides in Practically Valuable Chemical Reactions. *Russ. Chem. Rev.* **2016**, *85*, 248−279.

(6) Oshima, T.; Yokoi, T.; Eguchi, M.; Maeda, K. Synthesis and Photocatalytic Activity of $K_2CaNaNb_3O_{10}$, a New Ruddlesden−Popper Phase Layered Perovskite. *Dalton Trans.* **2017**, *46*, 10594−10601.

(7) Hu, Y.; Mao, L.; Guan, X.; Tucker, K. A.; Xie, H.; Wu, X.; Shi, J. Layered Perovskite Oxides and Their Derivative Nanosheets Adopting Different Modification Strategies towards Better Photocatalytic Performance of Water Splitting. *Renewable Sustainable Energy Rev.* **2020**, *119*, 109527.

(8) Badge, S. K.; Deshpande, A. V. Study of Dielectric and Ferroelectric Properties of Bismuth Titanate ($Bi_4Ti_3O_{12}$) Ceramic Prepared by Sol-Gel Synthesis and Solid State Reaction Method with Varying Sintering Temperature. *Solid State Ionics* **2019**, *334*, 21−28.

(9) Chen, C.; Ning, H.; Lepadatu, S.; Cain, M.; Yan, H.; Reece, M. J. Ferroelectricity in Dion−Jacobson $ABiNb_2O_7$ (A = Rb, Cs) Compounds. *J. Mater. Chem. C* **2015**, *3*, 19−22.

(10) Gomah-Pettry, J. Sodium-Bismuth Titanate Based Lead-Free Ferroelectric Materials. *J. Eur. Ceram. Soc.* **2004**, *24*, 1165−1169.

(11) Kuo, C.-Y.; Hu, Z.; Yang, J. C.; Liao, S.-C.; Huang, Y. L.; Vasudevan, R. K.; Okatan, M. B.; Jesse, S.; Kalinin, S. V.; Li, L.; et al. Single-Domain Multiferroic $BiFeO_3$ Films. *Nat. Commun.* **2016**, *7*, 12712.

(12) Weng, B.; Grice, C. R.; Ge, J.; Poudel, T.; Deng, X.; Yan, Y. Barium Bismuth Niobate Double Perovskite/Tungsten Oxide Nanosheet Photoanode for High-Performance Photoelectrochemical Water Splitting. *Adv. Energy Mater.* **2018**, *8*, 1701655.

(13) Xing, G.; Feng, Y.; Pan, M.; Wei, Y.; Li, G.; Dang, P.; Liang, S.; Molokeev, M. S.; Cheng, Z.; Lin, J. Photoluminescence Tuning in a Novel Bi^{3+}/Mn^{4+} Co-Doped La_2ATiO_6 :(A = Mg, Zn) Double

Perovskite Structure: Phase Transition and Energy Transfer. *J. Mater. Chem. C* **2018**, *6*, 13136−13147.
(14) Huang, D.; Dang, P.; Lian, H.; Zeng, Q.; Lin, J. Luminescence and Energy-Transfer Properties in Bi^{3+}/Mn^{4+}-Codoped Ba_2GdNbO_6 Double-Perovskite Phosphors for White-Light-Emitting Diodes. *Inorg. Chem.* **2019**, *58*, 15507−15519.
(15) Lerf, A. Storylines in Intercalation Chemistry. *Dalton Trans.* **2014**, *43*, 10276−10291.
(16) Wang, C.; Tang, K.; Wang, D.; Liu, Z.; Wang, L.; Zhu, Y.; Qian, Y. A New Carbon Intercalated Compound of Dion-Jacobson Phase $HLaNb_2O_7$. *J. Mater. Chem.* **2012**, *22*, 11086−11092.
(17) Uma, S.; Gopalakrishnan, J.; State, S.; Unit, S. C. Polymerization of Aniline in Layered Perovskites. *Mater. Sci.* **1995**, *34*, 175−179.
(18) Takeda, Y.; Suzuki, H.; Notsu, K.; Sugimoto, W.; Sugahara, Y. Preparation of a Novel Organic Derivative of the Layered Perovskite Bearing $HLaNb_2O_7{\cdot}nH_2O$ Interlayer Surface Trifluoroacetate Groups. *Mater. Res. Bull.* **2006**, *41*, 834−841.
(19) Guo, T.; Wang, L.; Evans, D. G.; Yang, W. Synthesis and Photocatalytic Properties of a Polyaniline-Intercalated Layered Protonic Titanate Nanocomposite with a P−n Heterojunction Structure. *J. Phys. Chem. C* **2010**, *114*, 4765−4772.
(20) Takeda, Y.; Momma, T.; Osaka, T.; Kuroda, K.; Sugahara, Y. Organic Derivatives of the Layered Perovskite $HLaNb_2O_7{\cdot}xH_2O$ with Polyether Chains on the Interlayer Surface: Characterization, Intercalation of LiCl, and Ionic Conductivity. *J. Mater. Chem.* **2008**, *18*, 3581.
(21) Ranmohotti, K. G. S.; Josepha, E.; Choi, J.; Zhang, J.; Wiley, J. B. Topochemical Manipulation of Perovskites: Low-Temperature Reaction Strategies for Directing Structure and Properties. *Adv. Mater.* **2011**, *23*, 442−460.
(22) Lagaly, G. Interaction of Alkylamines with Different Types of Layered Compounds. *Solid State Ionics* **1986**, *22*, 43−51.
(23) Constantino, V. R. L.; Barbosa, C. A. S.; Bizeto, M. A.; Dias, P. M. Intercalation Compounds Involving Inorganic Layered Structures. *An. Acad. Bras. Cienc.* **2000**, *72*, 45−50.
(24) Tahara, S.; Sugahara, Y. Interlayer Surface Modification of the Protonated Triple-Layered Perovskite $HCa_2Nb_3O_{10}\cdot xH_2O$ with n-Alcohols. *Langmuir* **2003**, *19*, 9473−9478.
(25) Aznar, A. J.; Sanz, J.; Ruiz-Hitzky, E. Mechanism of the Grafting of Organosilanes on Mineral Surfaces. IV. Phenylderivatives of Sepiolite and Poly (Organosiloxanes). *Colloid Polym. Sci.* **1992**, *270*, 165−176.
(26) Kimura, N.; Kato, Y.; Suzuki, R.; Shimada, A.; Tahara, S.; Nakato, T.; Matsukawa, K.; Mutin, P. H.; Sugahara, Y. Single- and Double-Layered Organically Modified Nanosheets by Selective Interlayer Grafting and Exfoliation of Layered Potassium Hexaniobate. *Langmuir* **2014**, *30*, 1169−1175.
(27) Yang, J.-M.; Luo, Y.; Bao, Q.; Li, Y.-Q.; Tang, J.-X. Recent Advances in Energetics and Stability of Metal Halide Perovskites for Optoelectronic Applications. *Adv. Mater. Interfaces* **2019**, *6*, 1801351.
(28) Kamminga, M. E.; Stroppa, A.; Picozzi, S.; Chislov, M.; Zvereva, I. A.; Baas, J.; Meetsma, A.; Blake, G. R.; Palstra, T. T. M. Polar Nature of $(CH_3NH_3)_3Bi_2I_9$ Perovskite-Like Hybrids. *Inorg. Chem.* **2017**, *56*, 33−41.
(29) Schaak, R. E.; Mallouk, T. E. Perovskites by Design: A Toolbox of Solid-State Reactions. *Chem. Mater.* **2002**, *14*, 1455−1471.
(30) Machida, M.; Mitsuyama, T.; Ikeue, K.; Matsushima, S.; Arai, M. Photocatalytic Property and Electronic Structure of Triple-Layered Perovskite Tantalates, $MCa_2Ta_3O_{10}$ (M = Cs, Na, H, and $C_6H_{13}NH_3$). *J. Phys. Chem. B* **2005**, *109*, 7801−7806.
(31) Wang, Y.; Wang, C.; Wang, L.; Hao, Q.; Zhu, X.; Chen, X.; Tang, K. Preparation of Interlayer Surface Tailored Protonated Double-Layered Perovskite $H_2CaTa_2O_7$ with n-Alcohols, and Their Photocatalytic Activity. *RSC Adv.* **2014**, *4*, 4047−4054.
(32) Rodionov, I. A.; Maksimova, E. A.; Pozhidaev, A. Y.; Kurnosenko, S. A.; Silyukov, O. I.; Zvereva, I. A. Layered Titanate $H_2Nd_2Ti_3O_{10}$ Intercalated with N-Butylamine: A New Highly Efficient Hybrid Photocatalyst for Hydrogen Production from Aqueous Solutions of Alcohols. *Front. Chem.* **2019**, *7*, 863.
(33) Nicolosi, V.; Chhowalla, M.; Kanatzidis, M. G.; Strano, M. S.; Coleman, J. N. Liquid Exfoliation of Layered Materials. *Science* **2013**, *340*, 1226419.
(34) Ida, S.; Ogata, C.; Eguchi, M.; Youngblood, W. J.; Mallouk, T. E.; Matsumoto, Y. Photoluminescence of Perovskite Nanosheets Prepared by Exfoliation of Layered Oxides, $K_2Ln_2Ti_3O_{10}$, $KLnNb_2O_7$, and $RbLnTa_2O_7$ (Ln: Lanthanide Ion). *J. Am. Chem. Soc.* **2008**, *130*, 7052−7059.
(35) Uppuluri, R.; Sen Gupta, A.; Rosas, A. S.; Mallouk, T. E. Soft Chemistry of Ion-Exchangeable Layered Metal Oxides. *Chem. Soc. Rev.* **2018**, *47*, 2401−2430.
(36) Takahashi, S.; Nakato, T.; Hayashi, S.; Sugahara, Y.; Kuroda, K. Formation of Methoxy-Modified Interlayer Surface via the Reaction between Methanol and Layered Perovskite $HLaNb_2O_7{\cdot}xH_2O$. *Inorg. Chem.* **1995**, *34*, 5065−5069.
(37) Shimada, A.; Yoneyama, Y.; Tahara, S.; Mutin, P. H.; Sugahara, Y. Interlayer Surface Modification of the Protonated Ion-Exchangeable Layered Perovskite $HLaNb_2O_7{\cdot}xH_2O$ with Organophosphonic Acids. *Chem. Mater.* **2009**, *21*, 4155−4162.
(38) Suzuki, H.; Notsu, K.; Takeda, Y.; Sugimoto, W.; Sugahara, Y. Reactions of Alkoxyl Derivatives of a Layered Perovskite with Alcohols: Substitution Reactions on the Interlayer Surface of a Layered Perovskite. *Chem. Mater.* **2003**, *15*, 636−641.
(39) Akbarian-Tefaghi, S.; Teixeira Veiga, E.; Amand, G.; Wiley, J. B. Rapid Topochemical Modification of Layered Perovskites via Microwave Reactions. *Inorg. Chem.* **2016**, *55*, 1604−1612.
(40) Jacobson, A. J.; Johnson, J. W.; Lewandowski, J. T. Intercalation of the Layered Solid Acid $HCa_2Nb_3O_{10}$ by Organic Amines. *Mater. Res. Bull.* **1987**, *22*, 45−51.
(41) Wang, Y.; Wang, C.; Wang, L.; Hao, Q.; Zhu, X.; Chen, X.; Tang, K. Preparation of Interlayer Surface Tailored Protonated Double-Layered Perovskite $H_2CaTa_2O_7$ with n-Alcohols, and Their Photocatalytic Activity. *RSC Adv.* **2014**, *4*, 4047−4054.
(42) Tahara, S.; Ichikawa, T.; Kajiwara, G.; Sugahara, Y. Reactivity of the Ruddlesden−Popper Phase $H_2La_2Ti_3O_{10}$ with Organic Compounds: Intercalation and Grafting Reactions. *Chem. Mater.* **2007**, *19*, 2352−2358.
(43) Liu, S.; Avdeev, M.; Liu, Y.; Johnson, M. R.; Ling, C. D. A New n = 4 Layered Ruddlesden−Popper Phase $K_{2.5}Bi_{2.5}Ti_4O_{13}$ Showing Stoichiometric Hydration. *Inorg. Chem.* **2016**, *55*, 1403−1411.
(44) Silyukov, O. I.; Minich, I. A.; Zvereva, I. A. Synthesis of Protonated Derivatives of Layered Perovskite-like Bismuth Titanates. Glas. *Phys. Chem.* **2018**, *44*, 115−119.
(45) Minich, I. A.; Silyukov, O. I.; Kulish, L. D.; Zvereva, I. A. Study on Thermolysis Process of a New Hydrated and Protonated Perovskite-like Oxides $H_2K_{0.5}Bi_{2.5}Ti_4O_{13}{\cdot}yH_2O$. *Ceram. Int.* **2019**, *45*, 2704−2709.
(46) Silyukov, O. I.; Kurnosenko, S. A.; Zvereva, I. A. Intercalation of Methylamine into the Protonated Forms of Layered Perovskite-Like Oxides $HLnTiO_4$ (Ln = La and Nd). Glas. *Phys. Chem.* **2018**, *44*, 428−432.
(47) Gopalakrishnan, J.; Uma, S.; Bhat, V. Synthesis of Layered Perovskite Oxides, $ACa_{2-X}La_xNb_{3-X}Ti_xO_{10}$ (A = K, Rb, Cs) and Characterization of New Solid Acids, $HCa_{2-X}La_xNb_{3-X}Ti_xO_{10}$ ($0 < x \leq 2$), Exhibiting Variable Bronsted Acidity. *Chem. Mater.* **1993**, *5*, 132−136.
(48) Nakato, T.; Nakade, M.; Kuroda, K.; Kato, C. Intercalation of N-Alkylamines into Perovskite-Related Layered Niobic Acid $HBiNb_2O_7{\cdot}nH_2O$. *Studies in Surface Science and Catalysis*; Elsevier, 1994; Vol. *90*, pp 285−290.
(49) Ida, S.; Okamoto, Y.; Matsuka, M.; Hagiwara, H.; Ishihara, T. Preparation of Tantalum-Based Oxynitride Nanosheets by Exfoliation of a Layered Oxynitride, $CsCa_2Ta_3O_{10-x}N_y$, and Their Photocatalytic Activity. *J. Am. Chem. Soc.* **2012**, *134*, 15773−15782.
(50) Xie, L.-Q.; Zhang, T.-Y.; Chen, L.; Guo, N.; Wang, Y.; Liu, G.-K.; Wang, J.-R.; Zhou, J.-Z.; Yan, J.-W.; Zhao, Y.-X.; et al. Organic-Inorganic Interactions of Single Crystalline Organolead Halide

https://dx.doi.org/10.1021/acsomega.0c00424
ACS Omega 2020, 5, 8158−8168

Perovskites Studied by Raman Spectroscopy. *Phys. Chem. Chem. Phys.* **2016**, *18*, 18112−18118.
(51) Vaia, R. A.; Teukolsky, R. K.; Giannelis, E. P. Interlayer Structure and Molecular Environment of Alkylammonium Layered Silicates. *Chem. Mater.* **1994**, *6*, 1017−1022.
(52) Ai-Jie, H.; Yu, Z.; Juan, G.; Yue-Fang, H.; He-Yong, H.; Ying-Cai, L. Interaction of Methylamine with Highly Siliceous MFI, FAU and FER-Type Zeolites. *Chin. J. Chem.* **2005**, *23*, 413−417.
(53) Wang, Y.; Nikolopoulou, M.; Delahaye, E.; Leuvrey, C.; Leroux, F.; Rabu, P.; Rogez, G. Microwave-Assisted Functionalization of the Aurivillius Phase $Bi_2SrTa_2O_9$: Diol Grafting and Amine Insertion: vs. Alcohol Grafting. *Chem. Sci.* **2018**, *9*, 7104−7114.
(54) Cattaneo, A. S.; Ferrara, C.; Marculescu, A. M.; Giannici, F.; Martorana, A.; Mustarelli, P.; Tealdi, C. Solid-State NMR Characterization of the Structure and Thermal Stability of Hybrid Organic−Inorganic Compounds Based on a $HLaNb_2O_7$ Dion−Jacobson Layered Perovskite. *Phys. Chem. Chem. Phys.* **2016**, *18*, 21903−21912.
(55) Kurnosenko, S. A.; Silyukov, O. I.; Mazur, A. S.; Zvereva, I. A. Synthesis and Thermal Stability of New Inorganic-Organic Perovskite-like Hybrids Based on Layered Titanates $HLnTiO_4$ (Ln = La, Nd). *Ceram. Int.* **2020**, *46*, 5058−5068.
(56) Shimizu, K.-i.; Itoh, S.; Hatamachi, T.; Kitayama, Y.; Kodama, T. Pillaring of Ruddlesden−Popper Perovskite Tantalates, $H_2ATa_2O_7$ (A = Sr or $La_{2/3}$), with n-Alkylamines and Oxide Nanoparticles. *J. Mater. Chem.* **2006**, *16*, 773.
(57) Wang, B.; Dong, X.; Pan, Q.; Cheng, Z.; Yang, Y. Intercalation Behavior of N-Alkylamines into an A-Site Defective Layered Perovskite $H_2W_2O_7$. *J. Solid State Chem.* **2007**, *180*, 1125−1129.
(58) Tsunoda, Y.; Sugimoto, W.; Sugahara, Y. Intercalation Behavior of N-Alkylamines into a Protonated Form of a Layered Perovskite Derived from Aurivillius Phase $Bi_2SrTa_2O_9$. *Chem. Mater.* **2003**, *15*, 632−635.
(59) Ida, S.; Ogata, C.; Unal, U.; Izawa, K.; Inoue, T.; Altuntasoglu, O.; Matsumoto, Y. Preparation of a Blue Luminescent Nanosheet Derived from Layered Perovskite $Bi_2SrTa_2O_9$. *J. Am. Chem. Soc.* **2007**, *129*, 8956−8957.

https://dx.doi.org/10.1021/acsomega.0c00424
ACS Omega 2020, 5, 8158−8168